

Scheduling Techniques of AI Models on Modern Heterogeneous Edge GPU - A Critical Review

Ashiyana Abdul Majeed and Mahmoud Meribout, *Senior Member, IEEE*

Abstract—In recent years, the development of specialized edge computing devices has significantly increased, driven by the growing demand for AI models. These devices, such as the NVIDIA Jetson series, must efficiently handle increased data processing and storage requirements. However, despite these advancements, there remains a lack of frameworks that automate the optimal execution of deep neural network (DNN). Therefore, efforts have been made to create schedulers that can manage complex data processing needs while ensuring the efficient utilization of all available accelerators within these devices, including the CPU, GPU, deep learning accelerator (DLA), programmable vision accelerator (PVA), and video image compositor (VIC). Such schedulers would maximize the performance of edge computing systems, crucial in resource-constrained environments. This paper aims to comprehensively review the various DNN schedulers implemented on NVIDIA Jetson devices. It examines their methodologies, performance, and effectiveness in addressing the demands of modern AI workloads. By analyzing these schedulers, this review highlights the current state of the research in the field. It identifies future research and development areas, further enhancing edge computing devices' capabilities.

Index Terms—accelerator, DLA, neural network, performance, scheduler.

I. INTRODUCTION

AS AI-System-on-Chip (AI-SoC) become increasingly popular and widely adopted in various embedded devices, it is vital to allocate the tasks in such a way that ensures high performance while operating under low power, particularly in edge devices [1]. One such powerful edge device is the NVIDIA Jetson series, which contains hardware accelerators that are well-adopted for AI and graphics applications. They comprise several hardware engines dedicated to various parallel computation models and interfaced with high-speed and low-power SDRAM memories. However, in most cases, these devices balance heavy workloads, including multiple DNNs, that can impair their performance. Some works consider optimizing the DNN execution in their GPUs, such as [2], but often overlook other accelerators, leading to suboptimal performance. Proper task scheduling and partitioning into their hardware engines can significantly enhance efficiency, thereby using the full potential of edge computing. Building schedulers remains challenging due to the heterogeneous nature of their hardware architecture and the unpredictable memory contention between different hardware engines. The contention arises from the use of a single shared bus connecting all the different hardware engines to the shared

SDRAM memory (Fig. 1). Hence, extensive work is necessary to develop these devices' scheduling and hardware partitioning algorithms.

With the rising demand for Jetson devices, it is of the utmost importance that a framework is developed to guarantee efficient and effective performance. For instance, the Jetson series has been used in autonomous driving. [3] evaluates the use of the Xavier and Orin device for pedestrian detection using an MM-Net model. Another example is a delivery robot that uses the Xavier device to navigate and reach the destination. Here, a modified single shot detector (SSD) is utilized for object detection [4]. Apart from robotics, the Jetson series has also been utilized for monitoring purposes, particularly in oceanography. Employing such devices offers researchers the ability to automate the process in a safe and more economical way, as opposed to traditional methods of physically measuring the data. It also gives them access to real-time data and insights [5]. Moreover, it has also been used in industrial inspection to recognize defects [6].

In each of these applications, implementing a scheduler would offer a more efficient, better utilized system. Ideally, the schedulers maximize the throughput, minimize latency and power consumption. However, satisfying these goals simultaneously is not trivial and so, most of the algorithms tend to optimize only few of them, while keeping the remaining above a threshold value. Another deciding factor in choosing the right scheduler is the number of DNN instances involved at the same time. Taking the case of the delivery robot [4], implementing a heterogeneity aware execution of concurrent deep neural networks (HaX-CoNN) scheduler would enable multiple DNN, each focused on different tasks, to be concurrently executed. For instance, the SSD was trained to identify people so another DNN like ResNet can detect the other obstacles. Allocating specific roles to DNN in this way can improve the system's performance as opposed to using a single, more generalized model. Moreover, using HaX-CoNN can improve latency by 20% over GPU-only execution, thereby increasing the efficiency of the system [7]. An alternative scheduler that could be utilized is the computational parallelization for CNNs (CP-CNN) scheduler, which allows the concurrent processing of frames for a single DNN model. CP-CNN can enhance the speed and efficiency of the SSD model by 75.6% and 75.9% respectively [8]. As AI models increase in complexity, it is vital to prioritize energy and latency in their performance. In fact, with the rise in use of large language models (LLM), there has been a renewed interest in the energy efficient execution of these models on the edge [9].

To date, no review paper has comprehensively compared

Ashiyana Abdul Majeed and Dr Mahmoud Meribout are with the Department of Computer and Information Engineering, Khalifa University, Abu Dhabi, UAE (email: 100059454@ku.ac.ae, mahmoud.meribout@ku.ac.ae).

the various schedulers for the recent NVIDIA Jetson edge accelerators. In [10], a survey on hardware and algorithmic optimizations for the old Jetson models was examined, namely the Jetson TK1, TX1, and TX2, where a DLA is absent. These algorithmic optimizations were limited to modifying the characteristics of the DNN used, including reducing the size of the DNN, image resolution, number of frames, and depth-map levels. Additionally, the same survey explored works that did consider leveraging both the GPU and CPU present in the Jetson devices to improve the performance of the DNN models, covering similar issues to those discussed in this paper, such as memory contention. Another review paper that dived into scheduling is [11], which considers training and inference workload scheduling for GPU data centers. It is similar to edge computing in terms of accelerator heterogeneity as they contain both CPU and GPU resources. Furthermore, there is also a resemblance in the approaches used for deep learning model training, where linear programming and performance modeling are popular in scheduling training jobs. This paper seeks to systematically compare various schedulers and their methodologies targeting more recent NVIDIA edge devices while also identifying areas for potential development.

II. BACKGROUND

A. Metrics

The performance of schedulers is assessed using three key metrics: throughput (T), latency (L), and utilization (U). The throughput refers to the amount of data a DNN model can process within a specific time frame, while latency refers to the time required to process a single input. Utilization evaluates the extent to which the processing power of the available accelerators is being employed. Various other values have been used in their problem formulation, as defined below:

- a_i represents a single task from a set A of all three DNN tasks and three recurrent neural network (RNN) tasks present in the Apollo autonomous driving software [12].
- ce_j represents a processing element from a set CE of all possible processing elements which include:
 - 2, 4, or 6 CPU cores.
 - 4 or 8 GPU cores.
 - 1 or 2 DLA units.
- $L[a_i, ce_j]$ represents the latency of a task a_i executed on the element ce_j .
- $B[a_i, ce_j]$ represents the binary decision as to whether or not the task a_i is executed on the element ce_j .
- N represents a DNN model.
- N_n represents a layer n present in a DNN N .
- $s(N_n)$ represents the element on which the layer N_n is executed.
- $L(N_n, s(N_n))$ represents the latency of a layer N_n executed on the element $s(N_n)$.
- TR_n represents the binary decision on whether a transition occurs at this layer N_n .
- $\tau(N_n, s(N_n), \text{OUT})$ and $\tau(N_{n+1}, s(N_{n+1}), \text{IN})$ represents the transition cost (time) for the layer N_n to exit the device $s(N_n)$ and for the layer N_{n+1} to enter the device $s(N_{n+1})$.

- $pipeline(N_n, s(N_n))$ represents the cost involved when the sub-unit executing the layer N_n is not the same as the previous layer N_{n+1} .
- $e(N_n, s(N_n))$ represents the energy consumed when executing layer N_n on the device $s(N_n)$. Similarly, the $e(N_n, s(N_n), \text{OUT})$ and $e(N_{n+1}, s(N_{n+1}), \text{IN})$ represents energy consumed for the layer N_n to exit the device $s(N_n)$ and for the layer N_{n+1} to enter the device $s(N_{n+1})$.
- ECT represents an energy consumption target the user sets.
- LT represents a latency target the user sets.
- $C_{N_n, s(N_n)}$ represents the slowdown on the layer N_n resulting from contention during the concurrent execution of the layers.
- P represents a performance objective set by the user.
- $size(F, I)$ represents the memory required for storing the immediate features from each inference stage, F , and the indicator matrix, I , which states whether these features are required in the following stage.
- M represents the maximum of the shared memory available to the processing elements.

B. Hardware Architecture of the Jetson AGX Devices

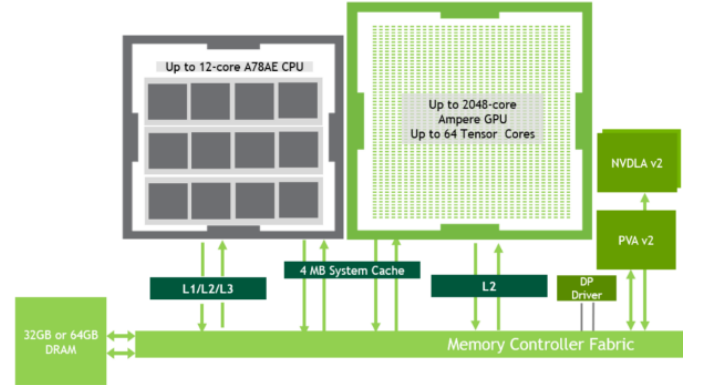


Fig. 1: Architecture of the NVIDIA Jetson AGX Orin [13]

The NVIDIA AGX Orin is able to provide almost 8 times the TOPS for AI and deep learning applications, compared to Xavier. For instance, using PeopleNet, the Orin device is able to produce 536 inferences per second, whereas Xavier is only able to output 196 inferences in the same period [13]. The NVIDIA Jetson AGX devices consist of the following modules:

- 1) **CPU:** The Orin device consists of 3 sets of 4 Cortex-A78 chips [13], as opposed to a Carmel CPU present in Xavier [14]. Apart from the three levels of cache, the system also includes a 4 MB system cache. The maximum operating frequency is 2.2 GHz [13]. It communicates with the memory using the system coherency fabric [15].
- 2) **GPU:** The Orin device uses an Ampere GPU [13] (rather than Volta in Xavier [14]), operating at a maximum frequency of 1.3 GHz. There are 16 streaming multiprocessors (SM) and two levels of cache present in

the device [13]. It is connected to the memory using the memory subsystem interface [15]. The GPU module alone can yield up to 170 Sparse TOPS to run AI models [16].

- 3) **Deep Learning Accelerator (DLA):** The DLA is essentially a fixed-function accelerator whose computational power is not comparable to GPU/CUDA but offers significantly higher energy efficiency. 2MB of SDRAM memory is dedicated for use by the DLA [17]. The Orin device houses a more recent version of the DLA than the Xavier device. The improvement increases the performance by a factor of 9, attributed to its architecture where a local buffer is introduced, and SDRAM bandwidth is reduced [13]. This is evident from Fig. 2.

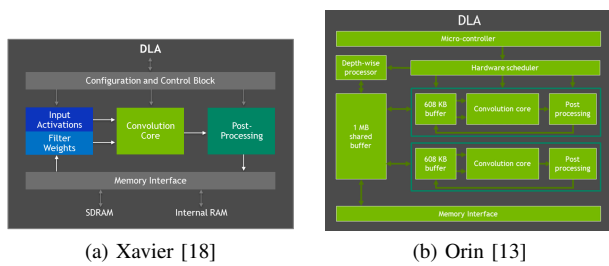


Fig. 2: Block diagram of the DLA

- 4) **Programming Vision Accelerator (PVA):** In both devices, the PVA consists of a Cortex-R5 chip, 2 direct memory access (DMA) engines, and 2 very long instruction word (VLIW) vector processing unit (VPU). The Orin device includes an L2 memory cache of 1MB in its PVA module [13]. It is adequate to handle relatively light, post-processing tasks like feature detection, stereo disparity, visual perception, feature tracking, and object tracking [14].
- 5) **Video Imaging Compositor (VIC):** This accelerator is responsible for pre-processing techniques like lens distortion correction, temporal noise reduction, and pixel processing [19]. The VIC in the Orin platform has a maximum frequency limit of 729.6 MHz [20], whereas in Xavier, it can reach up to 1036.8 MHz [21].

To the best of our knowledge, no paper has made use of the PVA and VIC module when scheduling tasks. Only [22] models the energy and memory contention between the CPU, GPU and PVA. This work could be extended to aid the scheduling algorithm to output the best execution pipeline. The PVA could be used for convolution layers and the VIC could be used to tackle pre-processing steps.

C. Software Development Kits and Libraries

NVIDIA provides resources that allow users to access the different modules present in the Jetson devices and execute tasks on the desired module. CUDA [23] and cuBLAS [24] libraries are still necessary for more complex parallelism in the multi-core system.

- **TensorRT:** It allows users to implement trained DNN models on the NVIDIA Jetson devices by building an

optimized inference engine. It allows users to alter techniques used in execution, such as mixed precision, and the option to choose the device for execution: GPU or DLA. TensorRT also offers inter-layer and intra-layer optimization techniques to ensure the best engine performance [25].

- **DeepStream:** It is built on top of other libraries, like TensorRT, to assist in developing AI applications. It can construct a complete setup from input to output for use in computer vision applications [26].
- **Vision Programming Interface (VPI):** It is a library that enables the use of image and video processing algorithms, allowing access to PVA and VIC. Some examples include image conversion, filtering, lens distortion correction, and feature tracker. It is part of the DeepStream SDK [27].

When executing tasks incompatible with the accelerator, the above resources redirect the task to be executed on the GPU. This can lead to interruptions if the GPU is already occupied for a different task. Furthermore, TensorRT does not allow for DNN convolution layers to be assigned to the PVA, limiting the use of the PVA for filtering and other pre-processing tasks.

D. Challenges of Building a Scheduler

When building a scheduler, certain challenges need to be addressed, which are listed below:

- 1) **Memory contention:** Memory contention occurs not only in the SDRAM and secondary memory but also within the cache and between the accelerators. As shown in Fig. 1, the Orin's GPU and specialized accelerators (including the DLA, VIC, and PVA) all share a common memory bus, the memory controller fabric, connected to an external LDDR5 SDRAM memory. Such a system necessitates careful management to ensure no conflict arises from accelerators simultaneously accessing this memory [7], [28]. A similar problem of a single memory bus is also present in edge tensor processing unit (TPU), explored in [29]. Here, the elements must wait if parameters are not cached, leading to an increase in memory traffic and, therefore, power consumption. When executing AI models, almost 50.3% of energy is spent on off-chip traffic [29]. Effective scheduling must account for these potential bottlenecks to optimize overall system performance.
- 2) **Transition cost:** When allocating layers to the appropriate accelerators, it is also vital to consider the possible latency incurred if consecutive layers are assigned to different devices. Data from the previous accelerator's memory must be transferred to the shared memory for the next accelerator to access the data. Hence, a latency is introduced, impacting the overall performance [7]. As such, running the consecutive layer on the same device in certain stages of the DNN may be more effective in avoiding the increasing latency. Thus, a trade-off needs to be made between the total transition time and the number of transitions that can occur in order to avoid compromising the performance of the DNN model.

- 3) **Accelerator properties:** Each accelerator has specific limitations concerning the tasks or layers it can handle, as well as the input/output formats it can accept. For example, depending on the function, the PVA and VIC are restricted to particular formats. The PVA can implement convolution and filter operations on unsigned integer 8-bit and 16-bit formats. In contrast, the VIC can implement image conversions and other manipulations on the same formats, usually on luma versions. The PVA's performance is close to or even faster than the CPU's for convolution. For instance, an unsigned integer 8-bit data of size 1920 by 1080 and a kernel of size three, the PVA takes 0.27 ms, whereas the CPU takes 0.297 ms [27]. The performance of VIC is faster than the CPU for rescaling and some remapping tasks. In rescaling a 640 by 480 image to 1920 by 1080, the VIC takes around 0.893 ms compared to the CPU which takes about 6.75 ms [30].

When looking at the DLA in particular, according to [31], some of the constraints include but are not limited to:

- Only FP16 and INT8 are supported. However, for certain layers, only one of these formats are supported. For example, the Equal operation is supported by INT8 alone. Slice and SoftMax operations are supported by FP16 only.
- For de-convolution layers, padding must be zero.
- Kernel sizes must range from 1 to 32.

In most cases, to ensure that the DLA is able to execute the portion of the DNN model, most schedulers [8], [32], [33] will allocate the beginning of the DNN model to the DLA as these layers tend to be the most compatible rather than the end of the DNN model. Hence, it is crucial to carefully consider layer specifications, input format, output format, and hardware limitations when assigning each layer to a device. This approach ensures compatibility and maximizes processing efficiency.

- 4) **Static versus Dynamic Schedulers:** Schedulers can be distinguished based on parallelization techniques as well as scheduling methods. Static schedulers follow a predetermined plan, whereas dynamic schedulers actively adjust the execution strategy in the run-time based on the performance metrics or the specific objectives defined by the algorithm. The aim could be minimizing latency, maximizing throughput, or reducing energy consumption, depending on the scheduler. While static schedulers are more straightforward to implement, they are inflexible when sudden changes occur during the execution pipeline. In such cases, dynamic schedulers are preferred. Almost all the schedulers referenced in this paper are static in nature, with the exception of dynamic heterogeneity aware execution of concurrent deep neural networks (D-HaX-CoNN) [7].
- 5) **Horizontal versus Vertical Schedulers:** In most cases, schedulers divide the layers present in the DNN model into sub-groups to be executed on the designated accelerator, which can be referred to as a vertical pipelining.

This can be ideal for the parallel processing of video frames and for multi-DNN execution. On the other hand, few schedulers consider dividing the DNN based on the width dimension such that each accelerator is able to independently execute a subset of the DNN model. This type of execution could be preferable for cases with a single DNN model.

III. SCHEDULERS

Schedulers developed for the NVIDIA edge devices can be categorized based on the methodology they use to find the optimal pipeline. They either use an optimization technique or a heuristic method to arrive at the solution. Most of the schedulers have been developed for the Xavier device. Since both Xavier and Orin device are similar architecturally, the schedulers are expected to function similarly.

A. Heuristic-based Scheduling Techniques

Most heuristic-based schedulers reach at the optimal configuration through an algorithm to find the best partitioning solution using a set of metrics that could involve latency, throughput, and power consumption.

1) **Jedi:** In Jetson-aware embedded deep learning inference (Jedi) [33], the solution is finalized when the algorithm reaches the highest throughput while maintaining a satisfactory utilization. This is done through a heuristic global search first, where a sample cut-point set allows the algorithm to locate an estimate cut-point, followed by a heuristic local search to determine the exact location of the cut-point. Additionally, a series of experiments, altering the following parameters, were carried out to attain the optimal combination for increasing the throughput:

- The number of threads for the operation of pre-processing and post-processing tasks where they are allowed to run concurrently to prevent bottlenecks from occurring (pre-processing and post-processing in Fig. 3). The number of threads is usually 1 or 2.
- The number of streams (referring to the sequence of operations performing the inference) of the assigned kernel (referring to the function) that can be run concurrently without performance saturation occurring (intra-PE parallelization in Fig. 3). Using the TensorRT framework, the number of streams ranges from 1 to 6.
- The number of stages the pipeline can be divided into for running on different devices (intra-network pipelining in Fig. 3). This can be a GPU-only execution, DLA-GPU or GPU-DLA-GPU.
- The application of partial network duplication (PND) is where the network portion is duplicated on the two DLA units and runs concurrently in the same stage, increasing the parallelism and utilization of the accelerators (PND in Fig. 3).

Fig. 3 shows how the above parameters are implemented in the overall pipeline to produce an execution timeline shown by Fig. 4. The Jedi scheduler does not tackle memory contention. However, it reduces memory requirements by opting for 8-bit integer or 16-bit float computation rather than 32-bit float [33].

This also has the additional benefit of complying with DLA requirements [31].

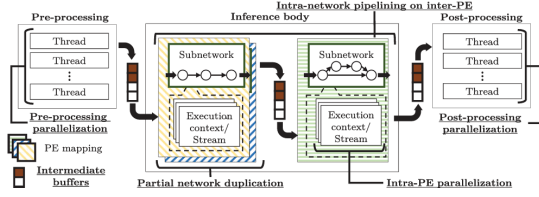


Fig. 3: Pipeline of the Jedi scheduler [33]

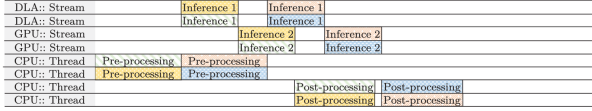


Fig. 4: Timing diagram of the model under Jedi scheme [33]

2) **CP-CNN**: CP-CNN [8] uses a different approach where the latency and computing power are the deciding factors in finding the partitioning point. The objective of CP-CNN is to ensure that the execution time in the GPU is equivalent to the execution time in the DLA, as shown in Fig. 5b. Fig. 5 compares the execution of multiple frames when using the GPU only and when using CP-CNN. The latency of the set of frames is reduced under CP-CNN with the implementation of the DLA and the concurrent processing. Since the DLA latency and GPU latency are equal, at no point in time are the DLA and GPU left idle. The CP-CNN algorithm iteratively compares the ratio of operations from the first till the current layer to the total operations in all layers (operation ratio) with the ratio of the computing power of the DLA to the total computing power (computing power ratio). The partitioning point is set as the current layer if the operation ratio is less than or equal to the computing power ratio. The algorithm also simultaneously compares the total time (operation time on DLA in addition to the data transfer time) required to execute these layers. If the latency to run till the partitioning point is more than the latency to run till the partitioning point with one additional layer, the partitioning point is incremented by one [8].

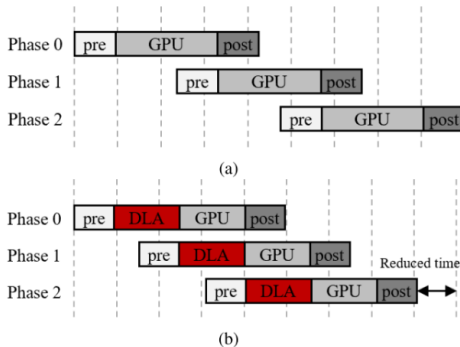


Fig. 5: Timing diagram of the model (a) under GPU execution alone (b) under CP-CNN scheme showing that it reduces overall latency [8]

3) **Herald and H2H**: Much like CP-CNN and Jedi algorithms, Herald [34] considers the concurrent execution of DNNs, but divides the layers and assigns them to the processing elements. A design-space exploration algorithm is implemented to assign layers based on data flow following which post processing is done to eliminate idle time. The heterogeneous model to heterogeneous system mapping (H2H) [35] builds on Herald while including transition costs as part of the layer assignment process. After performance modeling, the mapping algorithm follows four steps to complete the scheduling task. First, an initial mapping is generated based on assessing the layer-wise computation, while ignoring all other factors. From this mapping, weights are buffered to device's local SDRAM memory using a Knapsack algorithm. Adjacent layers are merged to further minimize the latency incurred from data transfer of input/output feature maps. Finally, the scheduler tries to compromise between transition and computation costs, resulting in a more transition-cost aware scheme. The dynamic version of the H2H scheduler uses a modified Knapsack algorithm [35].

B. Optimization-based Scheduling Techniques

1) **LP**: In contrast to most methods listed [1], [7], [8], [32], [33], linear programming (LP) methodology [36] maps the entire DNN instance onto a processing element, which can either refer to the sub-units or the whole accelerator (CPU, GPU or DLA). Since the DNN as a whole is executed on the processing element, transition points between layers are not considered. Within the multi-core CPU module, 2, 4, or 6 cores are considered using the OpenMP library [37]. For GPU module, 4 or 8 SM are considered using the CUDA and cuBLAS library [23], [24]. Using TensorRT [25], 1 or 2 units of the DLA are considered. The LP scheduler is built for use with the Apollo Autonomous Driving software [12], consisting of the following modules:

- Perception to locate objects.
 - DNN1 for object detection from a normal camera
 - DNN2 for object detection from a high resolution camera (excluded from the scheduling as it is too demanding for the Xavier device)
 - DNN3 for object detection from LiDAR sensors
 - DNN4 for object tracking
- Speech recognition (DNN5).
- Planning to plan the trajectory.
- Localization to receive position information from sensors.
- Map to provide road information.
- Prediction to predict future trajectory.
 - RNN1 for lane sequence-based prediction
 - RNN2 for obstacle status
 - RNN3 for probability lane sequence computation using the above two RNNs
- Control for command creation of accelerate, brake, steer, and other actions.
- A control area network (CAN) bus to command execution and information transfer.

These DNNs and RNNs are considered for scheduling and were evaluated to check for compatibility with the accelerators,

which clarifies that RNNs cannot be executed on DLA, and some DNNs cannot be executed on the CPU. Fig. 6 shows how the listed DNNs and RNNs are executed simultaneously in the Xavier device. The different neural network instances are executed recurrently based on a defined frame rate, making the scheduler static. The objective function of the LP scheduler focuses on minimizing the cumulative latency of the system (Equation 1).

$$\sum_{a_i \in A, ce_j \in CE} L[a_i, ce_j] \cdot B[a_i, ce_j] \quad (1)$$

The latency of each task was found through profiling on each device [36]. Memory contention was considered an assumption with a time factor added to the profiled timings. It does not consider the system's energy consumption.

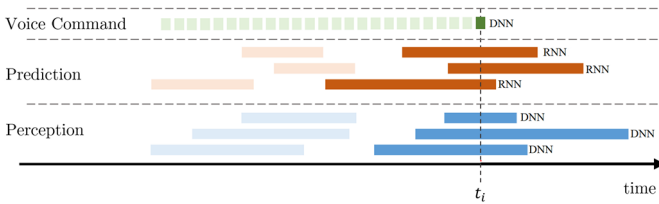


Fig. 6: Timing diagram of the DNNs and RNNs present in the Apollo software [36]

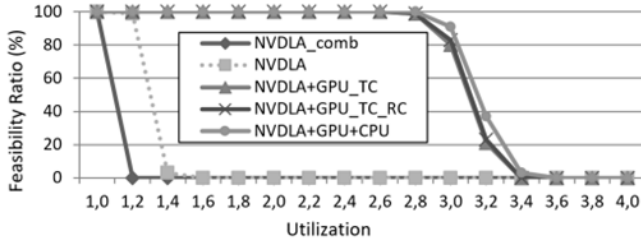


Fig. 7: Feasibility ratio versus utilization ratio with the LP scheduler on NVIDIA Jetson AGX Xavier [36]

The constraints include ensuring that a task a_i can only be mapped to a single processing element ce_j and that when a ce_j is chosen, some of the other values in the set CE become obsolete. For example, if both the DLA units are chosen for a single DNN instance, the individual DLA options are no longer considered for the remaining a_i present in A . Similarly, in the case of GPU, if all 8 SM are considered for a particular model, the 4 SM option is no longer present in the set CE [36].

Rather than presenting the throughput of the system during the concurrent processing, the scheduler is assessed on its success rate (feasibility ratio) of executing the DNNs and RNNs on the set of CE . Fig. 7 illustrates the effectiveness of the suggested method as it provides an improved pipeline, applying the DLA, GPU, and CPU in conjunction to ensure the completion of the workload effectively. Utilization ratio refers to the workload the devices can handle with respect to the workload that the combined DLA units can handle. For a ratio of 1, the system can handle (on average) 12 instances of DNN and RNN. As more devices are added to the set

CE , the feasibility ratio increases as the devices are able to schedule and handle the increased workload. Using DLA, GPU, and CPU, it is able to achieve a 100% feasibility rate in scheduling workloads 2.8 times the baseline capacity of the DLA. Thus, the LP method can apply heterogeneity to increase the workload and utilization of the Apollo system [36].

2) **AxoNN**: The energy-aware execution of neural networks (AxoNN) scheduler [32] follows a similar methodology to CP-CNN, dividing layers into DLA then GPU. AxoNN uses a constraint-based optimization problem focused on satisfiability along with empirical modeling. The energy, latency, pipeline, and transition times are found through performance modeling, shown in Fig. 8 and 9. A Z3 satisfiability modulo (SMT) solver is utilized to identify the ideal pipeline. The Z3 solver, developed by Microsoft, is intended for use in applications pertaining to software verification and analysis [38]. The same solver has also been used in the HaX-CoNN scheduler for a satisfiability (SAT) problem [7]. The objective function (Equation 2) aims to minimize the latency while ensuring that the energy consumed is below the threshold value set by the user.

$$\begin{aligned} \min \quad & \text{latency}(N, CE, S(N \rightarrow CE)) \\ \text{s.t.} \quad & \text{energy}(N, CE, S(N \rightarrow CE)) < ECT \end{aligned} \quad (2)$$

Equations 3 and 4 show how these values are calculated [32]:

$$\begin{aligned} \text{latency} = \sum_{n=0}^{\text{len}(N)} & \left(L(N_n, s(N_n)) \right. \\ & + TR_n \cdot \tau(N_n, s(N_n), OUT) \\ & + TR_n \cdot \tau(N_{n+1}, s(N_{n+1}), IN) \\ & \left. + TR_n \cdot \text{pipeline}(N_n, S(N_n)) \right) \end{aligned} \quad (3)$$

$$\begin{aligned} \text{energy} = \sum_{n=0}^{\text{len}(N)} & \left(e(N_n, s(N_n)) \right. \\ & + TR_n \cdot e(N_n, s(N_n), OUT) \\ & \left. + TR_n \cdot e(N_{n+1}, s(N_{n+1}), IN) \right) \end{aligned} \quad (4)$$

Fig. 10 shows that AxoNN could achieve an accuracy of 97.1% on execution time prediction and 98.2% on energy consumption prediction. In the worst-case scenario, the accuracy reduces to 78.1% and 71.9%, respectively. As mentioned previously, increasing the number of transitions not only involves an extra overhead of inter-layer performance but it also requires more time for the solver to suggest the optimal scheduler, going from five seconds for a single transition to a minute for three transitions on the Jetson AGX Xavier [32]. A comparison between the optimal schedule for a model and the GPU-only execution was absent from the paper as this would vary depending on the ECT set by the user.

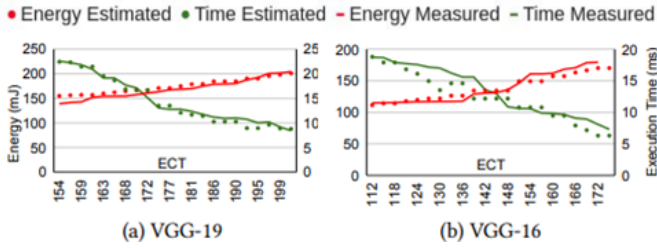


Fig. 10: Comparison between the actual and predicted (by AxoNN) performance and energy consumption of various CNN models on NVIDIA Jetson AGX Xavier where the horizontal axis represents the ECT [32]

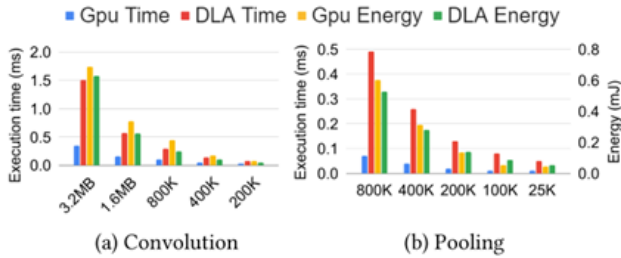


Fig. 8: Performance of convolution and pooling layers of VGG-19 based on execution time and energy consumption on NVIDIA Jetson AGX Xavier [32]

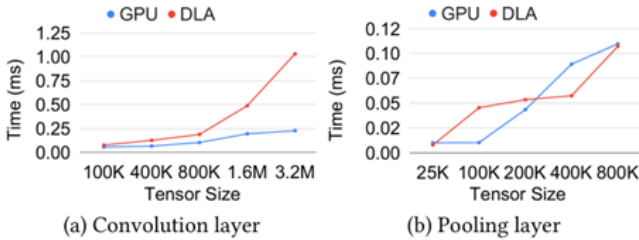


Fig. 9: Performance of convolution and pooling layers of VGG-19 based on transition time for different output sizes on NVIDIA Jetson AGX Xavier [32]

3) **GA**: Another approach explored in [1] involved using a genetic algorithm (GA) to schedule tasks based on profiling data from the different accelerators. Similar to AxoNN and HaX-CoNN, the transition and execution time are profiled before it passes to the GA. The GA then generates the ideal partitioning point for the DNN. The mechanism of the algorithm is similar to evolutionary processes in nature, where only the best-fit chromosome (an array of layers where the index represents the processing element) survives. The approach was initially tested on smartphones like the Galaxy S9, then later tested on the Xavier device in [33]. The objective of the GA scheduler when using a single DNN is to maximize the throughput and minimize the energy consumption. In the case of multiple DNNs, the objective is to minimize the latency and energy consumption. The GA method assigns layers of the DNNs to the processing elements. In this way, it is able to take advantage of parallelism within and between the processing units.

4) **HaX-CoNN**: HaX-CoNN [7] is similar to LP as it is scheduling multiple DNN. The difference is that LP uses linear programming to minimize latency, and HaX-CoNN uses a constraint-based satisfiability problem to minimize the latency or maximize the throughput (the objective changes depending on the application), as shown by Equation 5.

$$\begin{aligned} \max \quad & \sum_{i=0}^{len(DNN)} \frac{1}{latency(N, CE, S(N \rightarrow CE))_i} \\ \min \quad & \max latency(N, CE, S(N \rightarrow CE))_i \end{aligned} \quad (5)$$

Moreover, HaX-CoNN implements a switching technique between the DLA and GPU execution, as depicted in Fig. 11, which results in a swifter pipeline for the concurrent execution of DNNs. The CPU is not considered in executing tasks but rather to carry out the scheduling in the case of the D-HaX-CoNN. Similar to AxoNN, HaX-CoNN considers memory contention in terms of transition time. However, it differs from AxoNN and LP with the use of processor-centric contention-aware slowdown model (PCCS) [28] to further evaluate the effect of memory contention caused by the concurrent execution of layers. This is evident from Equation 6, where the value of $C_{N_n, s(N_n)}$ is found using PCCS, unlike AxoNN where *pipeline* value is from the profiling data alone [32].

$$\begin{aligned} latency = \sum_{n=0}^{len(N)} & \left(L(N_n, s(N_n)) \times C_{N_n, s(N_n)} \right. \\ & + TR_n \cdot \tau(N_n, s(N_n), OUT) \\ & \left. + TR_n \cdot \tau(N_{n+1}, s(N_{n+1}), IN) \right) \end{aligned} \quad (6)$$

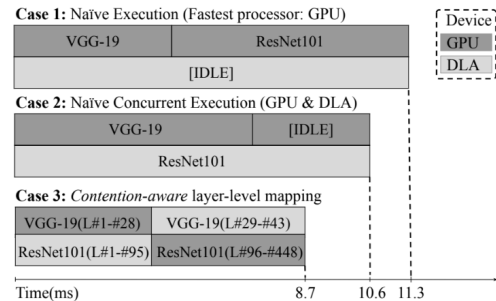


Fig. 11: Timing diagram of HaX-CoNN scheduling (case 3) compared to GPU-only (case 1) and GPU-DLA (case 2) [7]

Considering the application, HaX-CoNN can suggest optimal schedules for various types of DNN execution. The following were explored in [7]:

- Two instances of the same DNN running concurrently, improving the throughput up to 29% compared to GPU only and GPU-DLA execution.

- Two DNNs running simultaneously on either the same data or streaming data, improving latency and throughput by 23%.
- Three DNNs running where DNN1 and DNN2 are run one after the other while DNN3 runs parallel to both DNN1 and DNN2.

The dynamic version of the scheduler (D-HaX-CoNN) starts with an initial naïve schedule. With this, the concurrent DNN loop starts execution, and its schedule is updated with a more optimized version by the Z3 solver. The solver runs until the schedule can no longer be optimized. Fig. 12 shows the effectiveness of employing the D-HaX-CoNN scheduler, where it can come to the ideal solution in less than two seconds for the two systems with a pair of DNNs. There are a total of 3 changes in the graph. Part 1 is where GoogleNet and ResNet152 are run serially, while ResNet18 runs in parallel. Part 2 is where Inception and ResNet152 are run concurrently. Part 3 replaces Inception in the previous case with VGG19. In the case of the first part, the system has three DNNs, and therefore more layer groups and possibilities to consider. Moreover, the overhead of running the Z3 solver on the CPU, alongside the concurrent DNN execution in DLA and GPU, is less than 2% [7].

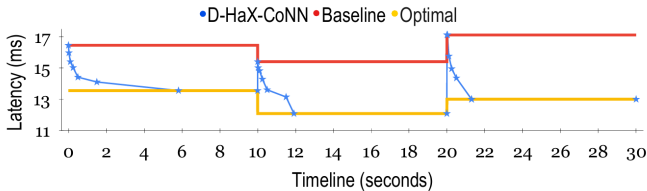


Fig. 12: Dynamic execution case where the system changes every 10 seconds [7]

5) **Map-and-Conquer**: Map-and-Conquer [39] follows a unique approach compared to all the schedulers mentioned above; firstly, it implements parallelism along the horizontal so as to divide the model into several independent inference stages that can run simultaneously, as opposed to the vertical pipelining (layer-wise). [40] argues that the division of layers across accelerators is not the most efficient way to utilize them. Operations, like convolution and multi-head self-attention, can be parallelized so that multiple operations of the same layer are concurrently carried out on different devices to maximize efficiency. Secondly, it is one of the first works to consider transformer models apart from DNN models, making it more versatile in terms of model architecture. Similar to GA, it uses an evolutionary algorithm to identify the ideal schedule, based on profiling data from TensorRT, and a predictor, XGBoost [41], to provide layer estimates of latency and energy on each of the devices to the algorithm. The predictor is required as it accounts for the computation and communication costs, similar to the PCCS model in HaX-CoNN. For VGG-19, compared to GPU-only execution, which consumes 630 mJ, Map-and-Conquer can provide a scheme with 136 mJ consumption (4.62x reduction) while keeping the latency relatively same (25 ms). The objective function of Map-and-Conquer is given by Equation 7.

$$\begin{aligned}
 &\min P \\
 &s.t. \text{ latency} < LT, \\
 &\quad \text{energy} < ECT, \\
 &\quad \text{size}(F, I) < M
 \end{aligned} \tag{7}$$

It allows the user to set an energy consumption threshold (similar to AxoNN), latency threshold and the performance objective, thus allowing for greater flexibility in the pipeline creation [39].

6) **MaGNAS**: The mapping-aware graph neural architecture search (MaGNAS) is another scheduler that uses an evolutionary algorithm, but developed for vision graph neural network (GNN). Compared to GPU-only execution, MaGNAS is able to reduce latency by a factor of 1.57 and increase efficiency by a factor of 3.38 on the Xavier device. It utilizes a two-step evolutionary algorithm, one to optimize the architecture of the GNN and another to carry out the layer mapping based on the performance modeling. During architecture optimization, the different generations of the architecture are evaluated on a fitness function that considers accuracy, latency and energy. After ranking them, some are eliminated and the remaining undergo mutation and crossover to get a new generation. The process continues until the search budget is reached. The same process is carried out for identifying the ideal hardware partitioning. Similar to Map-and-Conquer, it allows the user to set an energy consumption threshold and a latency threshold [42]. It does not consider the memory contention as part of the fitness function.

IV. COMPARATIVE ANALYSIS AND DISCUSSION

The difference between Jedi and CP-CNN is the idle time between the DLA and GPU. Fig. 4 and 5 illustrate this as in Jedi as there are instances in which either the DLA or GPU are left unused. However, in CP-CNN, this idle time is absent as the objective function aims to balance the DLA and GPU latency. As a consequence, the partitioning point for the same model varies. In Jedi, YOLOv3 is split into DLA and GPU at the 57th layer, whereas in CP-CNN, the split occurs at the 16th layer. On the other hand, Jedi makes use of both DLA units, unlike CP-CNN, where the DLA is taken as one whole unit. Moreover, Jedi is able to explore more instances of parallelization, both at the inter- and intra-accelerator level, compared to CP-CNN. In most cases, using Jedi, the number of streams for pre-processing varies from 1 to 6, and for post-processing, range from 1 to 3. The pipeline used the DLA with GPU in most cases, along with PND to use both the DLA units. A GPU alone was sufficient to infer smaller models, like YOLOv3 tiny in integer 8-bit format. Within the accelerator, the DLA implemented four streams while the GPU implemented two streams [8], [33].

AxoNN looks at the energy consumption along with the latency, using a threshold value. Even though CP-CNN considers the computing power as an objective parameter, it uses the power ratio, not the power value itself, as a determining

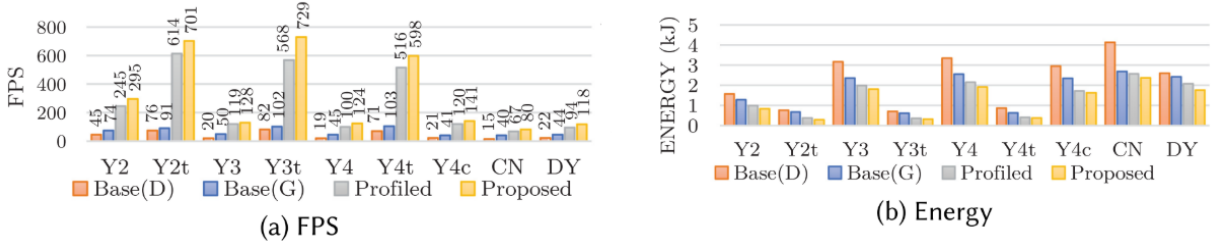


Fig. 13: Throughput and energy consumption of different DNN models when executed on Xavier using the schedulers. Y refers to the YOLO model, CN refers to CSPNet, and DY refers to DenseNet with YOLO. The performance of Jedi (proposed), is compared with profiled (GA) [1], DLA only (base(D)) and GPU only execution (base(G)). [33]

factor in locating the cut-point. It does not ensure that the optimal pipeline consumes the least energy. Additionally, another factor that differentiates the two schedulers is the processing. The CP-CNN allows for concurrently processing sequential frames in video streaming, unlike AxoNN that considers static images that cannot be processed simultaneously. Both AxoNN and CP-CNN explore the possibility of implementing more than a single transition. However, AxoNN opts for a single transition as there is an increased transition time caused by bottlenecks in the limited bandwidth. In CP-CNN, multiple transitions are considered for devices containing more than a single GPU [8], [32].

Table I compares the results for the execution of the YOLOv3 model using Jedi, GA and CP-CNN. The better performance of Jedi can be attributed to the horizontal parallelization occurring within the accelerators, emphasizing the importance of not just proper pipelining but also the need for multi-streaming. However, based on Fig. 13, the increasing throughput across the different models does not cause an increase in power consumption, which is usually not the case. Comparing the performance to CP-CNN, Jedi utilizes more of the resources with parallelization, causing a slight difference in energy consumption. Since the idle time is reduced in CP-CNN, it offers a more efficient and quicker pipeline. Overall, CP-CNN reduces the energy consumed per image by 62% to 84% while Jedi reduces the energy consumed for the entire set of images up to 55% [8], [33]. In the case of GA, unlike Jedi, it does not consider the use of multi-threading nor multi-streaming, which is the cause of its poor performance compared to Jedi, as shown in table I. Jedi provides a throughput increase of up to 32% and consumes less energy by up to 55%, compared to GA [33].

HaX-CoNN was able to outperform its heuristic predecessors, H2H [35] and Herald [34], as evidenced by table II. The difference in performance between HaX-CoNN, H2H and Herald arise from the fact that Herald and H2H do not consider memory contention as part of identifying the ideal partitioning point. Although H2H takes transition costs into account, this is not sufficient as the latency is impacted by the overhead incurred from the concurrent execution of DNNs.

Table III summarizes all the schedulers reviewed in this paper. Most studies aim to balance execution speed with energy efficiency. Generally, they employ a single data transfer from the DLA to the GPU, as frequent switches between these

TABLE I: Comparison of YOLOv3 execution on NVIDIA Jetson AGX Xavier

Scheduler	Performance metrics		
	Latency (ms)	Throughput (fps)	Energy / Image (mJ)
GPU-only [8], [33]	18.10-20.00	50-55	329-460
Jedi [33]	-	128	340
CP-CNN [8]	12.96	-	306
GA [33]	-	119	400

Note: The energy values for Jedi and GA were calculated approximately by dividing the energy by the number of images used for inference.

TABLE II: Comparison of VGG-19 with ResNet152 execution on NVIDIA Jetson AGX Xavier

Scheduler	Performance metrics	
	Latency (ms)	Throughput (fps)
GPU-only [7]	17.05	58
Herald [34]	19.73	50
H2H [35]	16.55	60
HaX-CoNN [7]	13.01	77

Note: The values are taken from [7].

devices introduce inefficiencies. This has proven to be one of the most efficient methods over constant switching between DLA and GPU. Only in rare instances is it preferred to use more than one transition, like in the case of CSPNet in Jedi. Additionally, most schedulers treat two DLAs as a single unit, and reducing inter-device transitions helps optimize speed. However, in the case of the Jedi scheduler, a PND was introduced, allowing two instances of the same network to run concurrently. The typical order of device operation places the DLA first, followed by the GPU, due to the nature of the task. The DLA is well-suited for early-stage tasks like feature extraction, while the GPU better handles later layers for specialized tasks like object detection or image recognition. The issue of layer compatibility of the DLA is reflected in the schedulers as well, where Jedi and CP-CNN are able to avoid this issue by implementing the transition point in the early part of YOLO models, which are otherwise not fully compatible with DLA. In the case of LP, AxoNN, and HaX-CoNN, the profiling stage ensures that the incompatible

TABLE III: Summary of the schedulers reviewed in this paper

Reference	Scheduler	Inter/Intra/Both	Static/Dynamic	Hardware	Execution	Methodology	Algorithm Aim
[36], 2019	LP	Both	Static	GPU, DLA, CPU (execute)	Multi-DNN	Linear programming model	Minimize overall latency
[1], 2020	GA	Both	Static	GPU, DLA, CPU (process)	Multi-frame	Parallelization within the accelerator and pipelining between the accelerator using a GA	Highest throughput with low energy consumption
[34], 2021	Herald	Inter	Static	GPU, DLA	Multi-DNN	Profiling followed by design-space exploration	Reduce latency
[34], 2021	Dynamic Herald	Inter	Dynamic	GPU, DLA	Multi-DNN	Profiling followed by design-space exploration	Reduce latency
[35], 2022	H2H	Inter	Static	GPU, DLA	Multi-DNN	Profiling followed by a set of algorithms to tackle transition cost and latency	Reduce latency and optimize weight locality
[35], 2022	Dynamic H2H	Inter	Dynamic	GPU, DLA	Multi-DNN	Profiling followed by a set of algorithms to tackle transition cost and latency	Reduce latency and optimize weight locality
[33], 2022	Jedi	Both	Static	GPU, DLA, CPU (process)	Multi-frame	Parallelization within the accelerator and pipelining between the accelerator	Highest throughput with satisfactory utilization
[32], 2022	AxoNN	Inter	Static	GPU, DLA	Single DNN	Empirical modeling with Z3 SMT solver	Minimize latency while ensuring energy consumption is within a threshold
[8], 2023	CP-CNN	Inter	Static	GPU, DLA, CPU (process)	Multi-frame	Parallel processing of sequential streaming data	Time to execute part on DLA = Time to execute part on GPU
[39], 2023	Map-and-Conquer	Inter	Static	GPU, DLA, CPU (execute)	Single DNN	Parallel processing of inference stages using evolutionary algorithm	Minimizes latency and energy consumption based on thresholds
[42], 2023	MaGNAS	Inter	Static	GPU, DLA	Single GNN	Two-step evolutionary algorithm	Minimizes latency and energy consumption based on thresholds
[7], 2024	HaX-CoNN	Inter	Static	GPU, DLA	Multi-DNN	Profiling followed by Z3 SAT solver	Maximizes utilization and reduces maximum latency
[7], 2024	D-HaX-CoNN	Inter	Dynamic	GPU, DLA, CPU (schedule)	Multi-DNN	Profiling followed by Z3 SAT solver	Maximizes utilization and reduces maximum latency

layers are permanently assigned to the GPU. Schedulers often use a looped structure to organize layer execution according to specific methodologies, with variations in the parameters used for decision-making. The Jedi method is distinguished by its multi-policy approach, while other schedulers assess each layer individually or as a group to seek transition points. In contrast, the LP method addresses the task as a whole, leveraging device heterogeneity by allocating different DNNs to each device. Finally, it is worth noting that transition costs were considered in schedulers developed after 2021, including H2H, AxoNN, CP-CNN, and HaX-CoNN.

V. CONCLUSION AND FUTURE PROSPECTS

This paper systematically compares the different schedulers developed for the more recent NVIDIA Jetson edge devices that include a DLA in its hardware. Overall, the general tendency is to develop schedulers that use optimization techniques with a single transition point between the DLA and GPU. Many determine the ideal schedule using the latency, with some including energy as part of their criteria. As numerous applications require more than a single DNN for execution, there is more emphasis in developing schedulers that can handle multiple DNN instances. Among schedulers, HaX-CoNN is remarkably versatile, accommodating diverse scheduling scenarios and Map-and-Conquer is adaptable in terms of model architecture.

As DNN models become increasingly complex, it is possible that the layers present at the beginning of the model may not always be DLA compatible. This may include padding in convolution transpose layer, which is present in many CNN-based generative adversarial network (GAN) models. Therefore, designing a system that can tackle such issues is beneficial by substituting the layers with similar operations before implementation. Current frameworks, like DeepStream and TensorRT, act defensively as they do not handle these issues and instead offload the CNN models as is to the GPU, resulting in pipeline disruptions. Hence, DNN model architecture needs to be studied before deploying the model on the edge. Additionally, it is essential to offload tasks or layers, where possible, to the unused PVA and VIC. In most literature, there is no mention of these devices being employed. One paper explored the relationship between energy and memory contention in CPU, GPU, and PVA [22], which could be utilized in schedulers to ensure an efficient use of PVA. A possible pipeline could involve VIC for pre-processing tasks like rescaling and image conversion, and PVA for initial convolutional layers or filter operations. However, NVIDIA's frameworks (DeepStream and VPI) limit the use of the PVA to tracking, filtering, and other pre-processing tasks. Using TensorRT, a DNN model's layers can only be assigned to the DLA or GPU [25], [43]. Another avenue to explore is the use of AI for scheduling. For instance, SCHED² [44] is a reinforcement learning technique to determine the best use of resources within a GPU data center. The same method can be applied to the edge devices, allowing for more dynamic scheduling that can foresee and adapt to any future information [11]. Ultimately, the choice of the scheduler must align with

the application in which it is implemented. In the case of multiple DNNs, it is better to opt for HaX-CoNN. With a single DNN carrying out real-time processing, CP-CNN and Jedi are ideal choices. If energy consumption is a concern, AxoNN and Map-and-Conquer are the better options.

REFERENCES

- [1] D. Kang, J. Oh, J. Choi, Y. Yi, and S. Ha, "Scheduling of Deep Learning Applications Onto Heterogeneous Processors in an Embedded Device," *IEEE Access*, vol. 8, pp. 43 980–43 991, 2020.
- [2] N. Capodiecici, R. Cavicchioli, M. Bertogna, and A. Paramakuru, "Deadline-Based Scheduling for GPU with Preemption Support," in *2018 IEEE Real-Time Systems Symposium (RTSS)*, Dec 2018, pp. 119–130.
- [3] H. Xu, S. Huang, Y. Yang, X. Chen, and S. Hu, "Deep Learning-Based Pedestrian Detection Using RGB Images and Sparse LiDAR Point Clouds," *IEEE Transactions on Industrial Informatics*, vol. 20, no. 5, pp. 7149–7161, May 2024.
- [4] S. Protasov, P. Karpyshev, I. Kalinov, P. Kopanov, N. Mikhailovskiy, A. Sedunin, and D. Tsetserukou, "CNN-based Omnidirectional Object Detection for HermesBot Autonomous Delivery Robot with Preliminary Frame Classification," in *2021 20th International Conference on Advanced Robotics (ICAR)*, 2021, pp. 517–522.
- [5] S. Martin, "Saildrone Charts Autonomous Oceanic Monitoring — resources.nvidia.com," 2023, (Accessed Apr. 17, 2025). [Online]. Available: https://resources.nvidia.com/en-us-jetson-success/saildrone-autonomous?lx=XRDs_y&ncid=no-ncid
- [6] Z. Zhang, C. Niu, Z. Zhao, X. Zhang, and X. Chen, "Small Object Few-Shot Segmentation for Vision-Based Industrial Inspection," *IEEE Transactions on Industrial Informatics*, pp. 1–12, 2025.
- [7] I. Dagli and M. E. Belviranlı, "Shared Memory-contention-aware Concurrent DNN Execution for Diversely Heterogeneous System-on-Chips," in *Proceedings of the 29th ACM SIGPLAN Annual Symposium on Principles and Practice of Parallel Programming*, ser. PPOPP '24. New York, NY, USA: Association for Computing Machinery, 2024, p. 243–256. [Online]. Available: <https://doi.org/10.1145/3627535.3638502>
- [8] D. Chun, J. Choi, H.-J. Lee, and H. Kim, "CP-CNN: Computational Parallelization of CNN-Based Object Detectors in Heterogeneous Embedded Systems for Autonomous Driving," *IEEE Access*, vol. 11, pp. 52 812–52 823, 2023.
- [9] X. Yuan, H. Li, K. Ota, and M. Dong, "Generative inference of large language models in edge computing: An energy efficient approach," in *2024 International Wireless Communications and Mobile Computing (IWCMC)*, May 2024, pp. 244–249.
- [10] S. Mittal, "A Survey on optimized implementation of deep learning models on the NVIDIA Jetson platform," *Journal of Systems Architecture*, vol. 97, pp. 428–442, 2019. [Online]. Available: <https://www.sciencedirect.com/science/article/pii/S1383762118306404>
- [11] Z. Ye, W. Gao, Q. Hu, P. Sun, X. Wang, Y. Luo, T. Zhang, and Y. Wen, "Deep Learning Workload Scheduling in GPU Datacenters: A Survey," *ACM Comput. Surv.*, vol. 56, no. 6, Jan. 2024. [Online]. Available: <https://doi.org/10.1145/3638757>
- [12] "Baidu Apollo Team, Apollo: Open Source Autonomous Driving," 2017, (Accessed Apr. 17, 2025). [Online]. Available: <https://github.com/ApolloAuto/apollo>
- [13] L. S. Karumbunathan, "NVIDIA Jetson AGX Orin Series," 2022, (Accessed Apr. 17, 2025). [Online]. Available: <https://www.nvidia.com/content/dam/en-zz/Solutions/gtc/t21/jetson-orin/nvidia-jetson-agx-orin-technical-brief.pdf>
- [14] "NVIDIA Jetson AGX Xavier System-on-Module Data Sheet," 2018, (Accessed Apr. 17, 2025). [Online]. Available: [https://developer.nvidia.com/embedded/downloads#?tx=\\$product.jetson_agx_xavier](https://developer.nvidia.com/embedded/downloads#?tx=$product.jetson_agx_xavier)
- [15] "NVIDIA Orin Series System-on-Chip Technical Reference Manual," 2023, (Accessed Apr. 17, 2025). [Online]. Available: [https://developer.nvidia.com/embedded/downloads#?tx=\\$product.jetson_agx_orin](https://developer.nvidia.com/embedded/downloads#?tx=$product.jetson_agx_orin)
- [16] "NVIDIA Jetson AGX Orin Series Data Sheet," 2023, (Accessed Apr. 17, 2025). [Online]. Available: [https://developer.nvidia.com/embedded/downloads#?tx=\\$product.jetson_agx_orin](https://developer.nvidia.com/embedded/downloads#?tx=$product.jetson_agx_orin)
- [17] "Hardware Architectural Specification — NVDLA Documentation," 2014, (Accessed Apr. 17, 2025). [Online]. Available: <https://nvdla.org/hw/v1/hwarch.html>
- [18] D. Franklin, "NVIDIA Jetson AGX Xavier Delivers 32 Teraops for New Era of AI in Robotics," 2018, (Accessed Apr. 17, 2025). [Online]. Available: <https://developer.nvidia.com/blog/nvidia-jetson-agx-xavier-32-teraops-ai-robotics/>

- [19] “NVIDIA Xavier Series System-on-Chip,” 2020. (Accessed Apr. 17, 2025). [Online]. Available: [https://developer.nvidia.com/embedded/downloads#?tx=\\$product,jetson_agx_xavier](https://developer.nvidia.com/embedded/downloads#?tx=$product,jetson_agx_xavier)
- [20] “Jetson Orin Nano Series, Jetson Orin NX Series and Jetson AGX Orin Series,” 2024, (Accessed Apr. 17, 2025). [Online]. Available: <https://docs.nvidia.com/jetson/archives/r35.5.0/DeveloperGuide/SD/PlatformPowerAndPerformance/JetsonOrinNanoSeriesJetsonOrinNxSeriesAndJetsonAgxOrinSeries.html#supported-modes-and-power-efficiency>
- [21] “Jetson Xavier NX Series and Jetson AGX Xavier Series,” 2024, (Accessed Apr. 17, 2025). [Online]. Available: <https://docs.nvidia.com/jetson/archives/r35.5.0/DeveloperGuide/SD/PlatformPowerAndPerformance/JetsonXavierNxSeriesAndJetsonAgxXavierSeries.html#supported-modes-and-power-efficiency>
- [22] M. A. H. Monil, M. E. Belviranlı, S. Lee, J. S. Vetter, and A. D. Malony, “MEPHESTO: Modeling Energy-Performance in Heterogeneous SoCs and Their Trade-Offs,” in *Proceedings of the ACM International Conference on Parallel Architectures and Compilation Techniques*, ser. PACT ’20. New York, NY, USA: Association for Computing Machinery, 2020, p. 413–425. [Online]. Available: <https://doi.org/10.1145/3410463.3414671>
- [23] “CUDA,” 2025, (Accessed Apr. 17, 2025). [Online]. Available: <https://docs.nvidia.com/cuda/cuda-toolkit-release-notes/index.html>
- [24] “cuBLAS,” 2025, (Accessed Apr. 17, 2025). [Online]. Available: <https://docs.nvidia.com/cuda/cublas/>
- [25] “Working with DLA,” 2025, (Accessed Apr. 17, 2025). [Online]. Available: <https://docs.nvidia.com/deeplearning/tensorrt/latest/inference-library/work-with-dla.html>
- [26] “DeepStream Documentation,” 2025, (Accessed Apr. 17, 2025). [Online]. Available: https://docs.nvidia.com/metropolis/deepstream/dev-guide/text/DS_Overview.html
- [27] “Convert Image Format,” 2024, (Accessed Apr. 17, 2025). [Online]. Available: https://docs.nvidia.com/vpi/algo_imageconv.html
- [28] Y. Xu, M. E. Belviranlı, X. Shen, and J. Vetter, “PCCS: Processor-Centric Contention-aware Slowdown Model for Heterogeneous System-on-Chips,” in *MICRO-54: 54th Annual IEEE/ACM International Symposium on Microarchitecture*, ser. MICRO ’21. New York, NY, USA: Association for Computing Machinery, 2021, p. 1282–1295. [Online]. Available: <https://doi.org/10.1145/3466752.3480101>
- [29] A. Boroumand, S. Ghose, B. Akin, R. Narayanaswami, G. F. Oliveira, X. Ma, E. Shiu, and O. Mutlu, “Google Neural Network Models for Edge Devices: Analyzing and Mitigating Machine Learning Inference Bottlenecks,” in *Proceedings of the 30th International Conference on Parallel Architectures and Compilation Techniques*, ser. PACT ’21. IEEE Press, 2024, p. 159–172. [Online]. Available: <https://doi.org/10.1109/PACT52795.2021.00019>
- [30] “Rescale,” 2024, (Accessed Apr. 17, 2025). [Online]. Available: https://docs.nvidia.com/vpi/algo_rescale.html
- [31] “Working with DLA - DLA Supported Layers and Restrictions,” 2022, (Accessed Apr. 17, 2025). [Online]. Available: https://docs.nvidia.com/deeplearning/tensorrt/archives/tensorrt-853/developer-guide/index.html#dla_layers
- [32] I. Dagli, A. Cieslewicz, J. McClurg, and M. E. Belviranlı, “AxoNN: energy-aware execution of neural network inference on multi-accelerator heterogeneous SoCs,” in *Proceedings of the 59th ACM/IEEE Design Automation Conference*, ser. DAC ’22. New York, NY, USA: Association for Computing Machinery, 2022, p. 1069–1074. [Online]. Available: <https://doi.org/10.1145/3489517.3530572>
- [33] E. Jeong, J. Kim, and S. Ha, “TensorRT-Based Framework and Optimization Methodology for Deep Learning Inference on Jetson Boards,” *ACM Trans. Embed. Comput. Syst.*, vol. 21, no. 5, Oct. 2022. [Online]. Available: <https://doi.org/10.1145/3508391>
- [34] H. Kwon, L. Lai, M. Pellauer, T. Krishna, Y.-H. Chen, and V. Chandra, “Heterogeneous Dataflow Accelerators for Multi-DNN Workloads,” in *2021 IEEE International Symposium on High-Performance Computer Architecture (HPCA)*. Los Alamitos, CA, USA: IEEE Computer Society, March 2021, pp. 71–83. [Online]. Available: <https://doi.ieeecomputersociety.org/10.1109/HPCA51647.2021.00016>
- [35] X. Zhang, C. Hao, P. Zhou, A. Jones, and J. Hu, “H2H: heterogeneous model to heterogeneous system mapping with computation and communication awareness,” in *Proceedings of the 59th ACM/IEEE Design Automation Conference*, ser. DAC ’22. New York, NY, USA: Association for Computing Machinery, 2022, p. 601–606. [Online]. Available: <https://doi.org/10.1145/3489517.3530509>
- [36] R. Pujol, H. Tabani, L. Kosmidis, E. Mezzetti, J. Abella, and F. J. Cazorla, “Generating and Exploiting Deep Learning Variants to Increase Heterogeneous Resource Utilization in the NVIDIA Xavier,” in *31st Euromicro Conference on Real-Time Systems (ECRTS 2019)*, ser. Leibniz International Proceedings in Informatics (LIPIcs), S. Quinton, Ed., vol. 133. Dagstuhl, Germany: Schloss Dagstuhl – Leibniz-Zentrum für Informatik, 2019, pp. 23:1–23:23. [Online]. Available: <https://drops.dagstuhl.de/entities/document/10.4230/LIPIcs.ECRTS.2019.23>
- [37] L. Dagum and R. Menon, “OpenMP: an industry standard API for shared-memory programming,” *IEEE Computational Science and Engineering*, vol. 5, no. 1, pp. 46–55, Jan 1998.
- [38] L. de Moura and N. Bjørner, “Z3: An Efficient SMT Solver,” in *Tools and Algorithms for the Construction and Analysis of Systems*, C. R. Ramakrishnan and J. Rehof, Eds. Berlin, Heidelberg: Springer Berlin Heidelberg, 2008, pp. 337–340.
- [39] H. Bouzidi, M. Odema, H. Ouarnoughi, S. Niar, and M. A. Al Faruque, “Map-and-Conquer: Energy-Efficient Mapping of Dynamic Neural Nets onto Heterogeneous MPSoCs,” in *2023 60th ACM/IEEE Design Automation Conference (DAC)*, July 2023, pp. 1–6.
- [40] R. Hadidi, J. Cao, M. S. Ryoo, and H. Kim, “Toward Collaborative Inference of Deep Neural Networks on Internet-of-Things Devices,” *IEEE Internet of Things Journal*, vol. 7, no. 6, pp. 4950–4960, June 2020.
- [41] T. Chen and C. Guestrin, “XGBoost: A Scalable Tree Boosting System,” in *Proceedings of the 22nd ACM SIGKDD International Conference on Knowledge Discovery and Data Mining*, ser. KDD ’16. New York, NY, USA: Association for Computing Machinery, 2016, p. 785–794. [Online]. Available: <https://doi.org/10.1145/2939672.2939785>
- [42] M. Odema, H. Bouzidi, H. Ouarnoughi, S. Niar, and M. A. Al Faruque, “MaGNAS: A Mapping-Aware Graph Neural Architecture Search Framework for Heterogeneous MPSoC Deployment,” *ACM Trans. Embed. Comput. Syst.*, vol. 22, no. 5s, Sep. 2023. [Online]. Available: <https://doi.org/10.1145/3609386>
- [43] “Gst-nvtracker,” 2025, (Accessed Apr. 17, 2025). [Online]. Available: https://docs.nvidia.com/metropolis/deepstream/dev-guide/text/DS_plugin_gst-nvtracker.html
- [44] Y. Luan, X. Chen, H. Zhao, Z. Yang, and Y. Dai, “SCHED²: Scheduling Deep Learning Training via Deep Reinforcement Learning,” in *2019 IEEE Global Communications Conference (GLOBECOM)*, Dec 2019, pp. 1–7.